Design, implementation and real-time digital control of a cart-mounted inverted pendulum using Atmel AVR Microcontroller

KASHIF ALTAF, ADEEL AKHTAR[1], SAEED-UR-REHMAN[2], JAVAID IQBAL[1]

Department of Electrical Engineering, COMSATS Institute of Information Technology, Islamabad
[1]College of EME, National University of Sciences & Technology, Rawalpindi
[2]Center for Advanced Research in Engineering, Islamabad
PAKISTAN

Abstract: - The paradigmatic inverted pendulum problem is one of the most important and favorite topics for Control System enthusiasts. A solution to this inherently unstable problem is discussed in this paper, with the pendulum being cart-mounted and the cart itself being moved by a belt spread between two pulleys. The pendulum is constrained to swing within predefined limits of ±25 degrees on either side of vertical axis. The feedback signals are cart and the pendulum positions using optical encoders. The digital control of the system is developed using an Atmel MEGA (ATMEGA) 8535 microcontroller. The user can tune the parameters of the system through a user interface provided in the form of a keypad and a Liquid Crystal Display (LCD). Mechanical aspects of the apparatus, electronic circuitry, control technique and experimental results are elaborated upon in the paper.

The apparatus is intended to be used as a general purpose Control Systems lab trainer to teach the characteristics of Proportional (P), Integral (I), Derivative (D), PI, PD and PID controls to electrical engineering students. Intuitive reasoning and an insightful approach to the control design are major emphasis of this effort.

Index terms: - Inverted Pendulum, Inherently unstable, cart-mounted, LCD, microcontroller.

1. Introduction

Control of inverted pendula is recognized as a benchmark problem for various controller designs and widely employed within laboratories for education and research purposes. It is popular for its simple setup and several interesting features such as the instability, nonlinearity and inherent non-minimum phase characteristics [1].

The previous approaches toward solving this complicated problem involved four categories:

- Category one ([2], [3], [4], [5]), simulation of inverted pendulum on a conveyor,
- Two ([6], [7], [8]), implementation of inverted pendulum on a cart,
- Three ([9], [10], [11], [12]), simulation of cart-mounted inverted pendulum,
- Four ([13]), implementation of cart-mounted inverted pendulum. According to our knowledge, the fourth category has been addressed the least, and no literature can easily be found in this category. We have adopted the fourth approach, and have partially linearised the problem by restricting the pendulum motion within 25 degrees on either side of the vertical balanced unstable position, and further simplified by restricting motion within a plane [14].

The object is a free-moving cart with an inverted pendulum attached to its upper surface through a pin. The feedback signals are cart position and pendulum angle from the vertical axis. These signals are fed to the controller in which PID control is implemented. The required driving signals are then fed to the motor.

The paper is arranged as follows: firstly the implementation with emphasis on mechanical model and electronic circuitry is presented. Then system modeling and control technique are discussed. Finally the experimental results show the feasibility of the proposed technique.

2. Physical Implementation

In this section we present the hardware and software implementation details. Our system stresses flexibility, portability and real-time tuning of parameters. The setup can feature a variety of schemes by allowing several factors to be changed to alter the natural response of the system, while maintaining compact size and low-weight. Moreover, the pendulum itself can be changed, compounded or made flexible [15].

The overall hardware is a few circuits for controllers and motor driving circuitry (H-Bridge), LCD, Keypad and a mechanical framework to support the cart-mounted pendulum and allow it move sideways on a track.

In order to achieve short-sampling periods for taking sensor readings, following factors need to be taken care of [13]:

- Sensors should be precise and fast in response

- Dynamic response of mechanical system should be optimized and servomotor should be able to provide small torque increments
- System should be synchronized and have high throughput without compromising communication reliability.

These three factors were very crucial, and have affected our choice of the required components and the overall design of hardware as well as software.

2.1 Sliding Mechanism

The most important thing in mechanical structure was the design of a low-friction rolling/sliding mechanism to move cart sideways. After a long hectic research, we ultimately decided to incorporate V-shaped bearings for their low rolling friction and greater stability they impart to the sliding platform they support. A combination of three v-bearings attached below the cart was used, with bearings fitted in a metallic slot from sideways so that play and backlash be minimized and cart could be kept from tilting to any direction. Pro-E drawings and actual assembly are shown below.

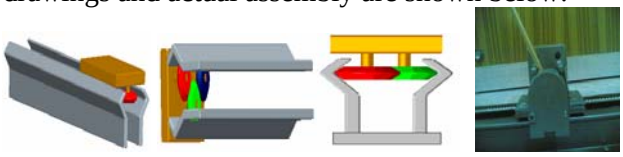

Fig.1 Pro-E models and actual sliding mechanism

The cart, fitted into a slot through V-shaped bearings, is also tied on both sides to a belt mounted on two gears. One of these gears is attached to actuating motor shaft and the other to the shaft of an optical encoder. The circumference of the gear having encoder is kept 10 times smaller than the distance between two gears (the whole length of the slot). In this way, when cart is on one end of the belt, encoder having 504 steps per revolution has zero count, and when on the other side, encoder has given 5040 counts. This is because ten turns have been made to move cart to this end of the belt.

Our mechanical structure has to overcome the rolling friction in the bearings of the cart and its inertia, and the air drag (negligible as compared to other forces). It has to accelerate it at sudden instants to and fro. To reduce internal overheads, this demands the use of coreless DC motor whose internal inertia is much less than the normal motors.

2.2 Motor

The motor used is a product of Buehler Motor GmbH [16]. This DC motor is coreless, rated at 12V and a no-load speed of 4000rpm, which is important to give adequate transient response. The peak torque is 300mNm which is enough, as calculated below, to provide enormous surges of acceleration for jerky motion.

2.2.1 Torque Calculation

The overall traction force is the sum of the force required to accelerate the cart, and the rolling friction (air drag neglected), where the former is

$$F1 = M.a \qquad (1)$$

M is the total mass of the cart with pendulum, and 'a' is the acceleration required.
The rolling friction is

$$F2 = C.M.g \qquad (2)$$

C is the coefficient of friction and is a function of the pressure applied on the surface, mass and gravitational acceleration, $(9.8\,m/s^2)$ and is roughly equal to 0.12 for our side bearings. The motor torque is then calculated by

$$T = F.r \qquad (3)$$

F is the traction force and r is the gear radius. Our cart and pendulum assembly weighs a total of almost 1kg and the radius of the pulleys is 3cm. The required acceleration is $2m/s^2$, yielding the following results: from (1), F1=2N, from (2), F2= 1.176 N, and total force F= F1+ F2= 3.176N. The required torque is calculated from (3) and comes out to be 95.28 mNm which is less than maximum torque of the motor, 300mNm. The conclusion is that the motor will easily provide the required peak torque without stalling.

2.3 Cart and sensor mounting

The cart is made in such a way so as to limit the maximum tilt of the fallen pendulum to 25 degrees on either side from the vertical axis. An optical encoder is attached to the pivot of the pendulum above the cart such that when the pendulum tilts, it also rotates the encoder shaft attached to the pivot, and we are able to know its angle through encoder feedback. The belt is mounted on a gear attached to the shaft of the motor. There is another encoder attached to the motor shaft, which tells us the position of the cart with respect to length of the slot. (For details on the operation of the incremental shaft encoder refer to [17]). If the cart reaches the either end during the balancing process and the pendulum is still tilted on the same side, the pendulum bob strikes the horizontal rod (intended for the same purpose), which pushes it back to the other side and the cart now automatically rushes back to the other side to balance it. In this way our cart never gets out of the predefined limits set on either side for the cart motion.

2.4 The mechanical assembly

The diagram of mechanical assembly made in Pro-Engineer, and its actual counterpart are shown below.

In Pro-E model, a simplified view of actual assembly is shown. The slot having cart rolling in it is not shown for sake of simplicity, but is shown in

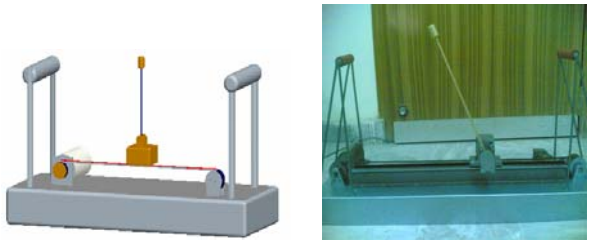

Fig.2 Pro-E model and actual apparatus

actual model. Its purpose is to avoid non-intended tilting of the pendulum and sagging of the belt, which might be caused due to cart's weight and could affect carts stability in vertical direction.

2.5 The user interface

To take values from the user for different parameters on the fly, an ATMEGA16 controller is interfaced to the main controller to relieve it from the tedious task of scanning the keypad and displaying the data on LCD, and hence avoiding any compromise on its performance as a compensator. The interface is through a serial RS-232 link at 9600 baud. When the user puts in the values through keypad, these are simultaneously sent to the main controller serially, and also to the LCD. The graphical LCD interfacing was much challenging. We used the LCD in "Graphics and Text XOR" mode. This mode takes the logical exclusive OR of each text and graphic pixel and the result determines whether to display pixel at that very position or not.

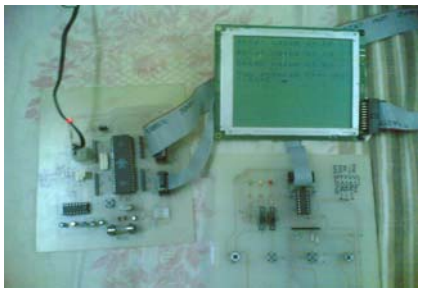

Fig.3 LCD, Keypad and controller board

2.6 Motor driving circuitry

Since our motor was drawing fairly high current, with an average of 4 Amps and peaks reaching up to 7 Amps, we designed motor drive for 15 Amps, keeping more than 100% margin of safety. It is designed with Bipolar Junction Transistors (BJTs) and is operated at 4 kHz. It is being controlled by the Pulse-Width-Modulation (PWM) channels on the ATMEGA8535 controller. The schematic diagram of the circuit is given below.

The motor drive (H-bridge) consists of four switches, upper two being PNP and lower two NPN. 2N3055 is a power transistor, TIP122 an NPN darlington and TIP127 a PNP darlington. TIP127/ TIP122 is connected to 2N3055 in darlington configuration to reduce required base current.

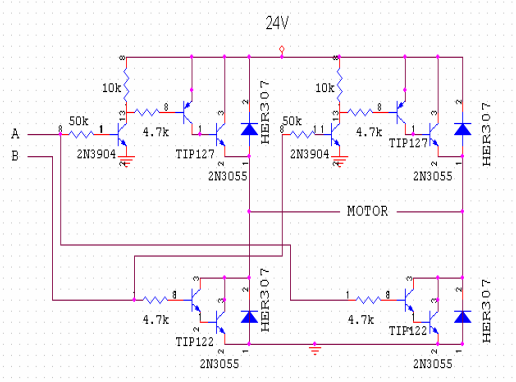

Fig.4 Schematic of Motor driving circuitry

The minimum beta for 2N3055 is 20, and for TIP122 and 127 it is 1000, thus making an equivalent beta of 20,000 minimum. The maximum possible value of collector current is 15A, and corresponding maximum base current is 0.75mA, which microcontroller can provide pretty easily.

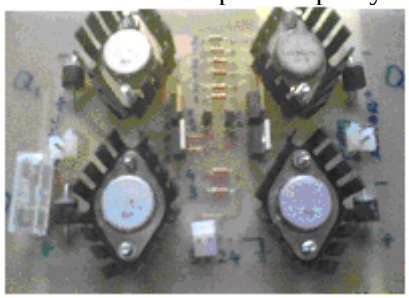

Fig.5 Actual H-Bridge

The four switches, while switching, are turned on and off in pairs. Each upper switch makes pair with the lower switch other than the one exactly below it. The bases of the switches in one pair are shorted together so these are turned on and off together. Thus we have a total of two control pins, one pin for each pair, and these are alternately turned on and off using two completely out of phase PWMs from PWM channels of controller. It is extremely necessary that these two pins should never be high simultaneously while the main power is being supplied to the bridge, because then, all the four switches would be turned on and the main power supply would be shorted, hence leading to a shoot-through situation which would ultimately burn the switches. While fast switching is taking place, residual currents in the switches after being turned off pose a threat to the performance of switches. To avert this problem, anti parallel diodes HER307 are used with all the four switches. Proper heat sinking is provided to all the four switches to facilitate cooling of the switches, and ultimately, the motor drive performed well even when 7-8 Amps were derived by the motor.

3. Controller Design

The proposed controller in this paper is a

PID controller for its robustness and convenience in tuning gains. The D-term improves the stability and the I-term removes the steady-state error. The gains of the system are chosen by hit and trial approach.

The idea is to keep the cart always moving, rather accelerating in the direction to the falling pendulum, so that a rapid vibratory motion of the cart occurs and the pendulum returns to its balanced state due to its inertia repeatedly. For example, when the pendulum is falling on the left side, the cart will be commanded to accelerate to the left, so that inertia brings pendulum back to right. Hence this repeating action causes a back and forth motion which keeps the pendulum swinging, with it amplitude of vibration reducing with each cycle towards zero, but never exactly reaching zero [18].

3.1 Parameters of the System

The physical parameters of the system are tabulated as follows:

Sr.	Symbol	Description	Value
1	M	Mass of the Cart	870 gm
2	m	Mass of the Pendulum	120 gm
3	b	Friction of the Cart	0.0 N/m/sec
4	I	Moment of Inertia	23.7 g-m^2
5	R	Radius of gear	3.0 cm
6	t	Time Constant of motor	0.5 second
7	K	Gain of Motor	18rad/sec/V
8	M	Gain of Feedback	1 V/rad/sec

Table 1: Physical parameters of system

3.2 Compensator Design

For compensator design, we have used the root-locus technique because it permits accurate computation of the time-domain response in addition to readily yielding frequency response information. The compensation of the system by the introduction of poles and zeroes is used to improve the operating performance. However, each additional compensator pole increases the number of roots of the closed-loop characteristics equation. The compensator in our case is PID controller. The parameters of the controller are set by hit and trial and by intuition of the user.

3.2.1 Transfer Function of the Whole System

Open loop and linearised transfer function for the whole (uncontrolled) system can be given as:

$$\frac{\Phi(s)}{E(s)} = K \frac{s}{(\tau_m s + 1)(\frac{s^2}{A_p{}^2} - 1)}$$

Where $\Phi(s)$ = Angular position of pendulum

$K = K_F K_P K_M r(M + m)$

$E(s)$ = Error voltage

3.2.2 Theme of our control

A common technique for meeting design criteria is root locus design. ***This*** approach involves iterating on a design by manipulating the compensator gain, poles, and zeros in the root locus diagram. The root locus diagram shows the trajectories of the closed-loop poles of a feedback system as a single system parameter varies over a continuous range of values. Typically, the root locus method is used to tune the loop gain of a Single-input-single-output (SISO) control system by specifying a feedback gain and the closed-loop pole locations. The root locus technique consists of plotting the closed-loop pole trajectories in the complex plane as gain varies. You can use this plot to identify the gain value associated with a desired set of closed-loop poles [19].

In our system, we introduce a pole at origin to cancel the effect of zero of the plant at the origin. The integral control will cancel the zero at origin. Now adding two zeros of the controller will provide finite terminus points to the two branches of locus on the left-hand side of the s-plane which were, otherwise, approaching to infinity.

3.2.3 Discretization of controller

PID controller in continuous domain is given by

$$U_c(t) = K_p e(t) + K_i \int e(t) + K_d \frac{de}{dt}$$

To discretize the controller, we need to approximate the integral and the derivative terms to forms suitable for computation by a computer [20]. From a purely numerical point of view, we can use:

$$\int_0^t e(t)dt \approx T_s \sum_0^t e(i)$$

$$\frac{de}{dt} = \frac{e(t) - e(t-1)}{T_s}$$

The discretized PID algorithm is therefore:

$$u(t) = K_p e(t) + \frac{K_c T_s}{T_i} \sum e(i) + K_c T_d \frac{e(t) - e(t-1)}{T_s}$$

3.2.4 Flowchart of algorithm

The overall flowchart of how the algorithm really works is shown below. First of all, error is calculated from the difference of past and present values of pendulum position. Then P component is calculated, I term calculated and added to the previous sum of I terms, and lastly, D term is computed. Derivate control component is saved to be used as an “old D term” in the next sample. Now the sum of these three components is calculated and fed to the actuator, and the whole process is repeated endlessly, as shown below.

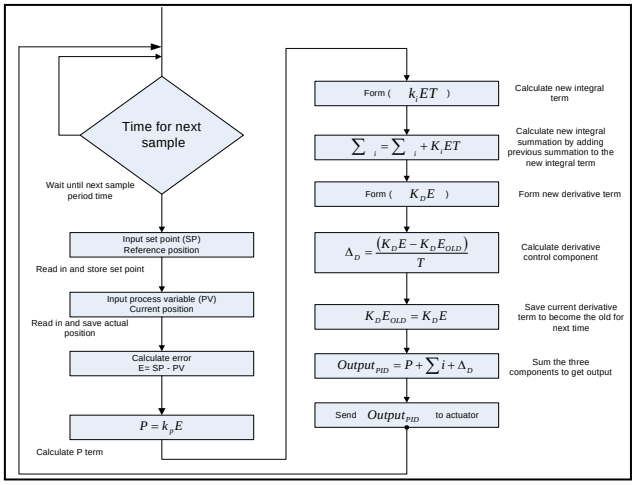

Fig.6 Flow diagram of the algorithm

3.2.5 Positional and Velocity PID Algorithms

Although the structures of the positional and velocity PID algorithms appear very different, they are in fact related [21]. The positional algorithm as derived is:

$$u(t) = K_p e(t) + \frac{K_c T_s}{T_i} \Sigma e(i) + K_c T_d \frac{[e(t) - e(t-1)]}{T_s}$$

Time shifting back by one sampling interval, we obtain

$$u(t-1) = K_p e(t-1) + \frac{K_c T_s}{T_i} \sum_{t=0}^{t-1} e(i) + T_d \frac{[e(t-1) - e(t-2)]}{T_s} + u_0$$

Subtracting this from the original, we end up with the velocity form, i.e.

$$u(t) = u(t-1) + K_c[e(t) - e(t-1)] + \frac{K_c T_s}{T_i} e(t) +$$

$$K_c T_d \frac{[e(t) - 2e(t-1) + e(t-2)]}{T_s}$$

This equation represents the PID control in velocity form.

3.2.6 Tuning of PID controller

Simulation based tuning of PID controller proved helpful and was quicker than hit and trial tuning. Effects of tuning P, I and D values on system response, as simulated in Simulink [22], are summarized below.

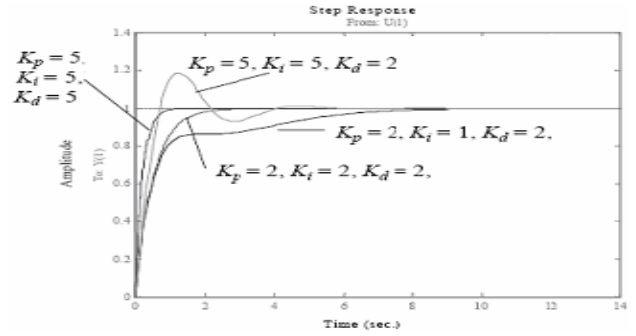

Fig.7 Effects of tuning P, I & D on response

4. Experimental results

4.1 Root Locus Diagram:

Root locus diagram of the system shows that the zero at the origin is cancelled by the pole at the origin. The two poles of the system, one from the right half plane and other from the left half plane come together and merge into the two zeros present in the left half plane.

The third pole of the system merges into the zero at infinity as gain is increased from zero to infinity. The compensator parameters at these values are $K_p = 8, K_i = 30, K_d = 1$

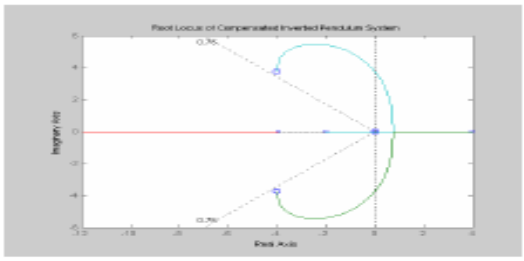

Fig.8 Root locus of compensated system

4.2 Impulse response

Impulse response of the PID compensated system is shown in following figure. The response of the system is observed to be very fast. The settling time is very small i.e. 0.028 s.

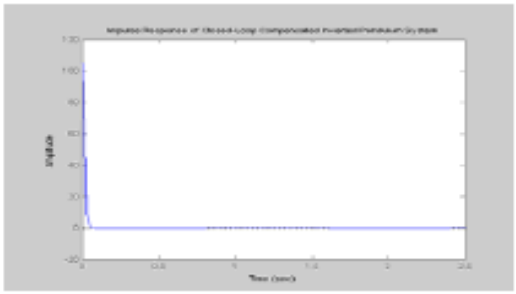

Fig.9 Impulse response of compensated system

4.3 Step response

The step response of the PID compensated system is shown in following figure. The DC Gain of the Closed-loop compensated system is 0.5 s. The percent overshoot is 8.48%. The steady-state error is almost zero.

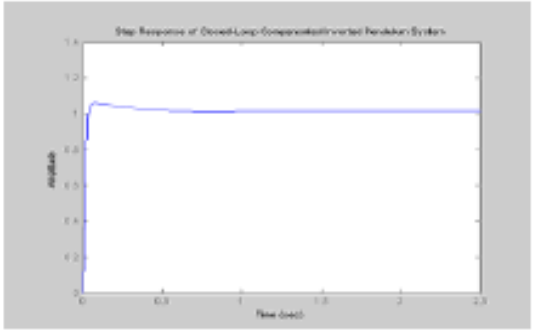

Fig.10 Step response of compensated system

5. Conclusion

This exercise provides a chance of designing a controller for a system that has a good dynamic behavior and hence the consideration for the transient response gains importance. The power of MATLAB and Simulink becomes more evident to one as all these designing would not have been possible without this tool.

One of the most difficult problems was the fabrication of a stable system with lesser backlash and play between motors and gears. The actuating motor with required specs was not available. We had to compromise over these specs to some extent. System performance could be much better if motor with exact specs were available. Moreover due to the negligence of the friction in the analysis of the system there is a small difference between the calculated parameters of PID controller and actual parameters required to stabilize the pendulum, but still the performance is pretty fine. The apparatus is good enough to give an insight into inverted pendulum mechanics and control, and the basic properties of P, I and D controls separately as well as in combination.

References:

[1] B. H. Shen and M. F. Hsieh, "Synchronous Control of the Parallel dual inverted pendulum system driven by linear servomotors", IEEE International Conference on Mechatronics, pp 157-161, Taiwan, 2005.

[2] Bastian, "Handling the non-linearity of a fuzzy logic controller at the transition between rules", Fuzzy Sets and Systems, vol. 71, pp. 369-387, 1995.

[3] G. A. Medrano-Cerda, "Robust control of inverted pendulum", IEEE Control Systems, pp. 58-67, June 1999.

[4] Leu, Wang and Lee, "Robust adaptive fuzzy neural controllers for uncertain non-linear systems", IEEE Transactions on Robotics and Automation, vol. 157, no. 5, pp. 808-817, October 1999.

[5] Chen, "Robustness design of non-linear dynamic systems via fuzzy linear control", IEEE Transactions on Fuzzy Systems, vol. 7, no. 5, pp. 571-585, October 1999.

[6] T. Yamakawa, "Stabilization of an inverted pendulum by a high speed fuzzy controller hardware system", Fuzzy Sets and Systems, vol. 32, no. 2, pp. 161-180, 1989.

[7] G. W. Linden and P. Lambrechts, "H infinity control of an inverted pendulum with dry friction", IEEE Control Systems, pp. 44-50, August 1993.

[8] J. Park and S. Lee, "Synthesis of control inputs for simultaneous control of angle and position of inverted pendulum", KITE Journal of Electronic Engineering, vol. 7, no. 3, September 1996.

[9] Widrow and Tolet, "Training of the cart-pendulum controller", IEEE transactions on Decision and Control, vol. 30, no. 6, pp. 452-465, 1987.

[10] Carnegie Mellon University and The University of Michigan, "Control Tutorials for Matlab: modeling an inverted pendulum" [online], Available at http://www.engin.umich.edu/group/ctm/examples/pend/invpen.html , 1997.

[11] A. Barto, R. Sutton, "Neuron-like adaptive element that can solve difficult learning control problems", IEEE Transactions on Systems, Man and Cybernetics, vol. SMC-13, no. 5, pp. 834-846, 1983.

[12] Teixeira, Zak, "Stabilizing controller design for uncertain non-linear systems using fuzzy models", IEEE Transactions on Fuzzy Systems, vol. 7, no. 2, pp. 133-142, April 1999.

[13] Fouad Mrad and Fadi Adlouni, "Real-Time control of free-standing Cart-mounted inverted pendulum using LABVIEW RT", IEEE, pp 1291-1298, 2000.

[14] Kent H. Lundberg and James K. Roberge, "Calssical Dual Inverted pendulum control", IEEE International Conference on Decision and Control, Hawaii, pp 4399-4404 2003.

[15] Ashab Mirza, Iram mahboob and Capt. Dr. Sarfraz Hussain, "Flexible Broom Balancing". AMSE Journal of C &D Simulation, Vol. 56, No 1, 2. 2001.

[16] http://www.buehlermotor.com [online]

[17] "US Digital Corporation Product Catalog", WA: www.usdigital.com, pp. 19-21, 45. Dec. 1999.

[18] Mario E. Magana and Frank Holzapfel, "Fuzzy Logic control of inverted pendulum with vision feedback", IEEE Transactions on Education, Vol. 41, No. 2, pp 165-170, 1998.

[19] Charles W. Anderson, "Learning to Control an Inverted Pendulum using Neural Networks", American Control Conference, Georgia, pp 31-37, 1988.

[20] Shiuh-Jer Huang and Chien-Lo Huang, "Control of an inverted pendulum using grey-prediction model", IEEE, pp 1936-1941, 1994.

[21] William J. Palm III, "Modeling Analysis and Control of Dynamic systems", 2nd Edition, John Wesley & Sons. Inc New York.

[22] F C Teng, "Real time control using Matlab Simulink", IEEE, pp2697-2702, 2000.